Enhancing the insulation capability of a vaccine carrier box: An engineering approach

(article starts on next page)

Enhancing the insulation capability of a vaccine carrier box: An engineering approach

Shitanshu Devrani [a,d,*], Rahul Tiwari [b], Naseef Khan [c], Krishnakumar Sankar [d], Shantanu Patil [d], K. Sridhar [d]

[a] *Department of Chemistry & Chemical Engineering, Chalmers University of Technology, Gothenburg 41296, Sweden*
[b] *Department of Mechanical Engineering, SRM Institute of Science & Technology, Kattankulathur 603203, India*
[c] *Department of Electrical & Electronics Engineering, SRM Institute of Science & Technology, Kattankulathur 603203, India*
[d] *Department of Translational Medicine & Research, SRM Medical College Hospital & Research Centre, Kattankulathur 603203, India*

A B S T R A C T

Being thermosensitive, Vaccines need storage at specific temperatures of 2-8 °C, and Vaccine Cold chain Carriers are the most widely utilized instruments to carry out rural vaccination drives in Low-income hot climate countries. Several developed designs for the carrier have reported superior performance, but their actual penetration into rural community medicine is limited due to reasons of cost and utility. Thus, the scope for improvement in the design is significant and it is also pertinent to quantify the effect of design features on the performance. Taking shared features possessed by such superior designs, the work presents the impact of geometry, vertically stacked vaccine tray assembly and usage of Phase Change Materials(PCM), on the final passive cooler assembly. A fabricated New Design with given features is cross-compared and analysed with a Market(Original) Design of the same scale and storage capacity. Analysis performed takes a scientific inclination towards Engineering and Insulation aspects of the Vaccine Box. It uses Conjugate Heat Transfer model(CFD simulations), Geometry analysis, experimentally derived Insulation R-values and Temperature monitoring to accomplish this. Secondly, the work presents a systematic design approach to improve upon the conventional design, PCM selection is made using DSC(Differential Scanning Calorimetry) testing, and Material of Construction(MOC) selection is made using Ashby plots based on the results of the simulations. Overall the Fabricated New Design gives an improvement of $\approx 16\%$ in R-value and $\approx 17\%$ improvement in the retention time of the specific temperature range, over the conventional (Original) Design.

1. Introduction

Vaccination and immunization form the backbone of public health in the modern world even more so now as the world population approaches an overwhelming figure of 10 billion. Primary vaccination drives in the global community rely on efficient cold chains for mass immunization. The current state of the cold chain, especially in the third world is far from idle or even satisfactory, with frequent reports of vaccines gone to waste due to improper storage and transportation [1, 2]. A widely attributed reason relates to the perishable potency of the standard vaccine package that requires precise temperature for storage which is not maintained especially at the end of the cold chain. With more than 271 vaccines in the market and a tenfold increase in patent applications since 1990s [3], World Health Organization (WHO) recommended standard package could comprise of the adjuvant vaccines such as Hepatitis B, Bascillus Calmette-Guerin(BCG), DTP(Diptheria,

Tetanus Toxoids and Tertussis), Tetanus Toxoid (TT) and Haemophilus-Influenzae Type B (Hib) [4,5]. These varied packages need ideal storage temperatures in the range of 2 to 8 °C, along with −2 to 2 °C and 8–12 °C subgroups that form the colder and warmer end of the storage range, respectively [6–8]. Several studies have shown the need for an improved cold chain and proposed management strategies for hot climate countries [4,9–11]. The underlying factors for this problem are many which dwell within the range of logistics, thermostability of vaccines, improper training of the staff, economics, ergonomics, and others. With the recent advancement in thermostable vaccines to inherently poses thermal resistance to sustain their potency, there are severe limitations and challenges [12,13]. These wider concerns make such vaccines a distant possibility especially when it comes to its application to hot-climate, low-income countries. Although the reasons for the failure in the cold chain could be varied, one of the most
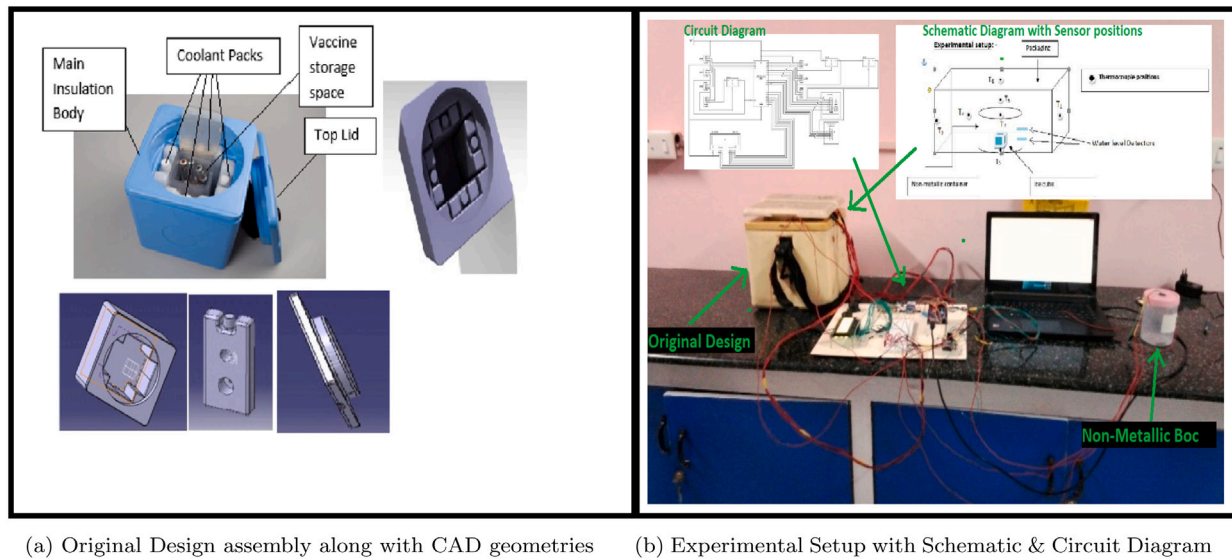
(a) Original Design assembly along with CAD geometries   (b) Experimental Setup with Schematic & Circuit Diagram

Fig. 1. Details of the experimental setup.

commonly identified reason is the limitations of the vaccine carrier box for rural delivery by the virtues to its design and applicability.

Since 1986, there has been at least a 15 fold increase in vaccine costs [3] and WHO has seen a 25% increase [14] in yearly dosage which subsequently promotes reliance on robust cold chains. Thus, a more efficient vaccine carrier design is cardinal to the system, not only does it improve vaccine potency lifetime but a consistent and reliable design offers varied opportunities when it comes to planning logistics and ergonomics. With such incentives and scope for improvement, several approaches like [7,15,16] utilized an approach relying on using commercial Phase Change Material(PCM) and conventional insulation assemblies to come up with an off-grid passive cooling setup. Besides, various composite PCM materials for cold storage systems have also been tested [17]. Another upgraded design utilizes thermoelectric plates(Peltier effect) aided cooling that yields a semi-passive cooling assembly [18–20]. Other designs for portable refrigeration systems rely on solar-powered vapour-compression & absorption cycles [21,22]. However, their limitations are its inconveniently larger sizes for the last stages of the cold chain. Various strides in integrating portable thermoelectric coolers to such carriers have resulted in proprietary technology such as [23,24]. This is evidence that a thermo-responsive Peltier cooling system that dynamically stabilizes the temperature could be an appropriate approach to maintain cold chains in hot-climate low-income countries. Efforts to progress in this direction have been provided with products like Nano-Q by Savsu Technologies [25], Colli-Pee/ COOL-VAX [26], PVSD [27] that have been extensively tested to give a 2–3 fold enhancement in the vaccine safe keeping time compared to conventional market designs. Common features shared by these superior designs is its cylindrical outer body casing and mostly a vertically aligned tray stacking system which might be coupled with a semi-passive cooling system. Despite this, clear gaps in the literature to define the role of factors such as the external geometry, internal vaccine stacking system and Material of construction(MOC) on the overall insulation capacity of the vaccine carrier still persist. Further, the choice of PCM determines the thermal inertia; however, their role in combination with the before mentioned aspects is largely unexplored. Discussions on the overall improvement in ergonomics and optimization practices using heat transfer modelling and experimental verification are given by [28–31].

This work provides a comprehensive study performed purely from a Physics & Engineering aspect. Further, it provides a comparison between a typically employed conventional design(referred to as 'Original Design', Fig. 1(a)) with a fabricated prototype of a cylindrical 'New

Table 1
Mass, Momentum and Energy equations used for the simulation in Section 2.1.1.

Equation type	Variable	Diffusion coefficient	Source term
Mass	1	0	0
X-Momentum	u	μ	$-\nabla_x P + S_b$
Energy	T	$\frac{\mathcal{K}}{C_p}$	$S_e = \beta T \frac{\partial p}{\partial t} + Q''' + \mu \phi$

Design'(Referred as such) of similar capacity. This work builds from the earlier work(briefly covered in Section 3.1[32]) where the 'Original Design'(used for immunization programs at SRM Hospital, India) was studied and evaluated in detail. It is important to note that although there are various designs very close to the one fabricated for this study, the investigators aim to narrow down the impact of critical design features on insulation capability of the vaccine box.

2. Materials & methods

The work on improving the cold insulation properties is performed to increase the vaccine potency retention time, which directly correlates to reducing heat transfer gradients within the vaccine carrier and minimize heat penetration. Initially, steady-state heat transfer modelling leading to transient analysis(Section 2.1) is done to study heat penetration into the original design, followed by experimental data obtained from temperature monitoring and R-value test(Section 2.4). With the results obtained, a similar approach to design and model a PCM encapsulated tray-based new design along Section 2.2) and Tray MOC(Material of Construction)(Section 2.3) selection is made. Finally, the R-value test is performed to evaluate(Section 2.4) and cross-compare the results from the original design.

2.1. Heat transfer modelling

2.1.1. Geometry analysis

Passive cooling systems focus on minimizing heat transfer from its surroundings to the cooled area inside; it follows naturally that such a packaging system should expose the least surface area for the volume occupied. The sphere should be an ideal shape for such a container package, but due to the impracticality of managing such a design, a cylindrical design is proposed that is easier to manage and carry [7]. To investigate the heat transfer trends around such a cylindrical design against a cube(original design's geometry), ANSYS Fluent is used for an analysis based on the governing equations described in Table 1. The

3-D geometry is treated as an impenetrable hollow solid with an outer thickness of the material taken to be HDPE(High-Density Polyethylene) while the inner space for both systems is treated to be air at 0 °C. The incoming fluid is set to be air(with its default properties) with the flow velocity of 5 m/s at 50 °C along the x-axis. The prime purpose of this simulation is to compare and establish an overall geometry for the new design(cylindrical) when compared to the existing original design(cubical).

2.1.2. Conjugate heat transfer modelling

Computational Fluid Dynamics (CFD) Tool FLUENT, which is part of the ANSYS workbench package, is used to perform steady-state leading towards transient conjugate heat transfer analysis on the interior of the assembly with a focus on convective and conductive modes of heat transfer. This analysis excludes radiation mode of heat transfer since the aim is to simulate the interior environment of the completely closed vaccine box which has no exposure to sunlight. This passive cooling interior environment is directed by the continuity equation (1), the momentum equation (2), and the energy equation (3) with a source term(G) based on sensible and latent heats of the PCMs. These are given as:

$$\frac{\partial \rho}{\partial t} + \sum_{i=1}^{3} \frac{\partial(\rho u_i)}{\partial x_i} = 0 \tag{1}$$

$$\frac{\partial(\rho u_i)}{\partial t} + \sum_{j=1}^{3} \frac{\partial}{\partial x_j}(\rho u_j u_i) = -\frac{\partial P}{\partial x_i} + \sum_{j=1}^{3} \frac{\partial(\tau_{ij})}{\partial x_j} + \rho f_i \tag{2}$$

$$\frac{\partial T}{\partial t} + \frac{v \nabla T}{\rho C_p} = \frac{k}{\rho C_p} + G \tag{3}$$

$$where, \ G = m C_p \Delta T + m \lambda \tag{4}$$

To save on the computational time, the basic assumptions made are steady-laminar airflow, isotropic and homogeneous material properties in the system. Besides, radiation and gravitational forces are neglected, also the mesh geometry was simplified. However, it is a common observation from reality that the utility of the box is to take out vaccines at the rural immunization drive or post. This would require the box lid to be opened to retrieve vials on a reasonably regular basis disrupting the internal environment. Hence to simulate and take this physical practicality into account, a User Defined Function (UDF) code as a boundary condition is plugged in(See 3.4.1 & Appendix G).

2.2. Selection of a suitable PCM

PCM selection is crucial to maintaining a favourable temperature over prolonged periods for a passive cooling assembly. Their incorporation in the system increases thermal inertia, and it is only imperative that the most appropriate PCM should have the maximum possible latent heat energy within the temperature range required(0 °C–8 °C). Based on this and [15,33], four potential candidates are selected namely Gelfrost, Medicool, 1-Decanol and Tetradecanol(procured from Kalyani Pvt.Ltd., Medicool', Merck', respectively) for Differential Scanning Calorimetry(DSC) testing. TA Instruments D100 DSC is utilized to study energy absorbed (endotherm) as a function of temperature to characterize the melting-freezing process cyclically. Each sample crucible is subjected to cyclic heating/cooling rates of $\pm180, \pm250$ and ±276 J/s for 3 h to vary the temperature from -2 °C to 12 °C and vice-versa.

2.3. Selection of MOC for the vaccine tray

First constraints on the MOC selection is that it must have reasonable tensile and impact strength as the application demands the tray to withstand rough use and impact from the inner walls of the vaccine box. The hollow tray is a replacement for conventional coolant packs from the original design and should contain a PCM to maintain the

Table 2
Stage 1,2, 3 Constraints applied along critical properties.

Property	Minimum	Maximum
Tensile strength (MPa)	20	–
Fracture toughness (MPa a.m 0.5)	1	–
Melting point (°C)	80	
Thermal conductivity (W/m °C)	0.1	0.7
Water absorption @ 24 hrs (%)	–	0.05
Price ($/kg)	–	3

Table 3
Stage 4 Constraints applied along critical properties.

Environmental impact	Minimum	Maximum
Embodied energy recycling (MJ/kg)	–	75
CO2 Footprint in current supply (kg/kg)	–	1.7

vaccine temperature in the range of 0 °C-8 °C. The tray should provide passive cooling by removing heat from the vaccines and at the same time resist heat flow from the environment, implying a suitable thermal conductivity for the MOC. It should also be reasonably crystalline with a moderately high glass transition temperature(T_g) as it could be exposed to temperatures from -10 °C to 45 °C. Additionally, the material used should be lightweight, implying minimum density and water-resistant as condensate can form inside the vaccine case. The product should be reusable for over several cycles making its environmental impact and cost secondary constraints. Ashby plots are constructed by applying constraints to important properties using the software CES EDUpack 2018. The first stage is to compare tensile strength per density and thermal conductivity, stage two & three is to apply constraints for important properties (Table 2). Stage four is to apply constraints for environmental impact(Table 3).

2.4. Experimental evaluation

R-value test has proven to be a reliable metric or quantification standard used in the cold chain industry [2,30,34] to access the insulation capacity or the Heat resistance value of packaging equipment. A setup to monitor temperatures at various locations inside a closed box is devised to evaluate the overall performance of the vaccine carrier box and perform the R-value test within this setup. Briefly, R-value test quantifies the resistance value to heat flow of any packaging or insulation equipment, the principle applied is that 454 grams (1 lb.) of water at 32 °C absorbs 151.9 kJ(363 Kcal) of heat to melt [34,35].

The test setup consists of the vaccine cooler(Original or New Design) with 6 thermocouple (DS18B20) probes inside. Within the vaccine storage space, a non-metallic(plastic) box with 100 g($\approx$ 100 ml) ice and two water level sensor(at 3 cm and 6 cm heights) probes is placed. Additionally, the inside lining of the non-metallic container has aluminium foil sheets and a 7th temperature sensor inserted. All the readings from 9 sensors (7 temperature, 2 water level) are stored. The activation of the second water level sensor(at 6 cm) marks the end of the R-value experiment as it signifies that all bulk ice has melted to water. The microcontroller used here is Atmega 2560(Arduino Mega)coded to sense the temperature and water level readings against time. Data display and logging is done on a LCD screen and stored in a 16 GB memory stick(Fig. 1(b)). The closed setup is allowed to rest at room temperature of 24 °C. The timer in the system noted temperature readings within the box from the placed sensors at 30-second intervals. Following established equations that have been devised to calculate the R-value are utilized to process the data obtained [34].

$$\text{System R-value} = \frac{(\text{Box Area})(\text{Temperature Difference})}{(\text{Melt Rate})(\text{Latent Heat})} \tag{5}$$

R-value obtained for different packages is fitted to an empirical formula which takes into account the contribution of conduction, convection and radiation.

$$R - value = 0.27th + 0.26np + o.56nf (\pm 20\%) \tag{6}$$

Table 4

Constraints applied along critical properties on the Original Design.

Parameter	Boundary conditions
Outside ambient temperature	T = 43 °C
Inside vaccine space temperature	T = 6 °C
Coolant body temperature	T = 0 °C
Convective heat transfer of air coefficient(Outside)	h = 11 W/(m² K) at T = 43 °C
Convective heat transfer of air coefficient(inside)	h = 1 W/(m² K) at T = 6 °C
Latent heat of PCM(Water)	λ = 323 kJ/(kg)

where *th, np, nf* represent the average wall thickness(in cm), number of plain surfaces and the number of aluminium foil surfaces, respectively. Eq. (6) helps analyse the contributions of conduction, convection and radiation into total penetration of heat.

$$\text{Ice Required} = \frac{(\text{Box Total Surface Area})(\text{Temperature Difference})}{(\text{R-value})(\text{Latent heat})} \quad (7)$$

Ice requirement calculations can be done once the R-value is decided for the package using Eq. (7).

3. Results

3.1. Evaluation of the original design

The conventional designs used are mostly thick insulated boxes with wastercoolant packs inside(Fig. 1(a)). A Polyurethane foam (35 to 60 mm thickness) lined with an internal polystyrene coating provides the core insulation. The main body is externally coated with an HDPE lining. The specimen box used for the analysis is a 1.6-litre capacity Vaccine box carrier by Apex international (specifications provided in Appendix C). Details of the results for this section have been summarized from [32].

To perform thermal simulations on the original design as per Section 2.1.2, the CAD model is created using CATIA(V5,Dassault Systems) as shown in Fig. 1(a) and further simulated upon. The most critical boundary conditions applied are given in Table 4, these are chosen on the assumptions that a vaccine casing could be exposed to peak summer temperatures of 43 °C, correspondingly the inside passive water coolants are precooled to be at 0 °C possessing unique latent melting capacity. Due to the virtues of design, the majority of heat transfer inside the casing is expected to be attributed to convection due to which inside air temperature is initially at 6 °C and the convective heat transfer coefficients at the temperatures involved become significantly important. The corresponding contour for the interior region of the carrier is presented in Fig. 2(b), it clearly shows significant excessive heat penetration from the bottom of the vaccine carrier as taken at a time interval of 22 h(additional details are provided in Appendix D).

The experimental procedure described in 2.4 section is used to draw verification of trends from the simulation. Each thermocouple($T_1 - T_7$) attached has been named accordingly in the schematic diagram (Fig. 2(a)) of the setup and the corresponding Temperature (° C) vs Time (h) plot at each point has been highlighted in Fig. 2(a). The important conclusion drawn from this is that within 26 h the temperatures for all the sensors placed within the box surpasses the temperatures for safekeeping of vaccines (2–8 °C). Most notably readings for the base sensor (T_5), large temperature fluctuations over time are consistently observed. This fluctuation points towards temperature gradients developed within the box leading to thermal shocks which limits the duration of vaccine safe keeping time ($\approx$ 26 h for 24 °C ambient temperature). This significant and rapid heat transfer from the base is in line with simulation profile from the Fig. 2(b). Previous work confirms

the same [15,36], and this stems from continuous heat conduction through contact with the ground leading to thermal gradients generated within the system.From Eq. (5) & (6), R-Value of 4.724 is calculated with individual contribution to heat transfer being 51.43% conduction, 27.51% Convection and 23.7% radiation. From (7), the minimum ice requirement of 300 g is calculated for a system operating for 72 hrs. at 43 °C.

3.2. Results of geometry analysis

Considering Section 2.1.1, geometrical analysis of shape concerning its potential for cold insulation is conducted. The original cubical design is compared with the proposed cylindrical new design. Fig. 3 represents the heat distribution from incoming air at 50 °C over a cubical 3(a) and cylindrical 3(b) geometry across the cross section.

Figs. 4(a) & 4(b) show graphical representations of the simulated temperature profiles across the length of the lines 1, 2, 3 & 4 (in Figs. 3(a) & 3(b)). These lines are the 2-D representations of the planes cut across the two bodies, namely cuboid and cylindrical. As can be observed, there is a steep and substantial decrease in the temperature at the bulk of the cylindrical body; this decrease is consistently lower across all lines when compared to the cuboidal geometry. Cylinder bulk temperature goes all the way from 50 °C to minimum 11.2 °C 4(b) whereas the minimum bulk temperature for cuboidal geometry is 14.5 °C 4(a). Increase of internal temperatures is due to the advection of the incoming air at 50 °C and its interaction with the surface of the geometries. As can be observed from Fig. 4, the cuboid geometry consistently offers higher heat penetration than the cylindrical bulk body across all lines which is a direct consequence of cylinder's lower Surface Area to Volume ratio(lowest after a Sphere) than a Cuboid [7,24,26]. These results formed the primary motivation to pursue a cylindrical design for the vaccine carrier(See Appendix E for velocity contours).

3.3. PCM selection

Four distinct PCMs in line with the selection criteria as per Section 2.2 are selected. The DSC curves for the four PCMS are shown in Fig. 5(a). The differential areas between the curves and the baseline are calculated from ORIGIN software. As can be seen from Fig. 5, all 4 potential candidates seem to show some form of area under the curve in the range of 0° to 8 °C which is indicative of melting in this range. From 5(a), the curve for Medicool is an indicator of meagre latent heat of vaporization offered making it an apparent elimination. Further, looking at curves for Gelfrost and Tetradecane, both offer significant area under the curve from the baseline. However, since Gelfrost offers melting at the lower end of the range, i.e. between −2 to 5 °C while Tetradecane offers a very sharp and rapid melting across a very narrow temperature range of 5 to 7 °C, this makes the two candidates unsuitable for this application. As can be seen for 1-Decanol, a significant area under the curve signifies a more spread out melting over a range of 0 to 6 °C making it a suitable candidate for the choice of PCM.

Fig. 5(b) shows the calculated area of 3.40487 and further latent enthalpy for melting is calculated to be 276 kJ/kg. This is consistent with results from studies by [37,38] on 1-Decanol along with other PCMs (Methanol, 1-Pentanol, Paraffin and Tetradecanol) that reported similar results.

3.4. Conjugate heat transfer analysis for the new design

Based on the conclusions from Sections 3.1, 3.2 & 3.3, cylindrical tray design with compartments for water and 1-Decanol is developed. This cylindrical vaccine tray has an outer diameter of 6 cm, and inner diameter as 3 cm, water is filled in the outer compartment while 1-Decanol fills inside the inner compartment. The combination of these
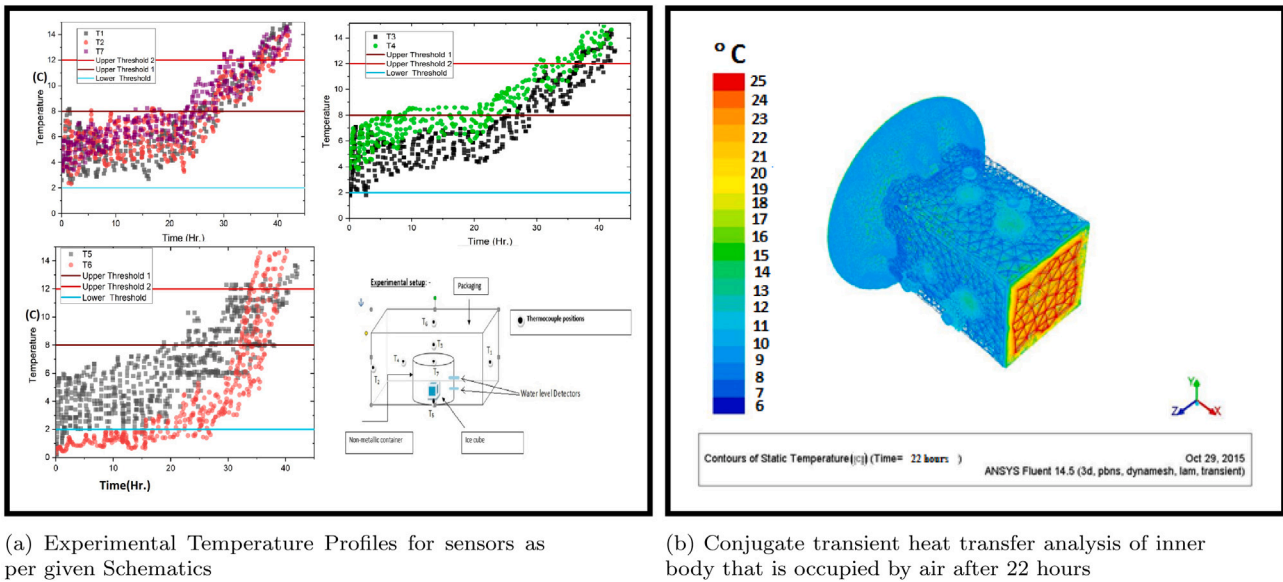
(a) Experimental Temperature Profiles for sensors as per given Schematics

(b) Conjugate transient heat transfer analysis of inner body that is occupied by air after 22 hours

Fig. 2. Results from heat transfer simulation.

(a) Top view of Heat distribution over a cuboid

(b) Top view of Heat distribution over a cylinder
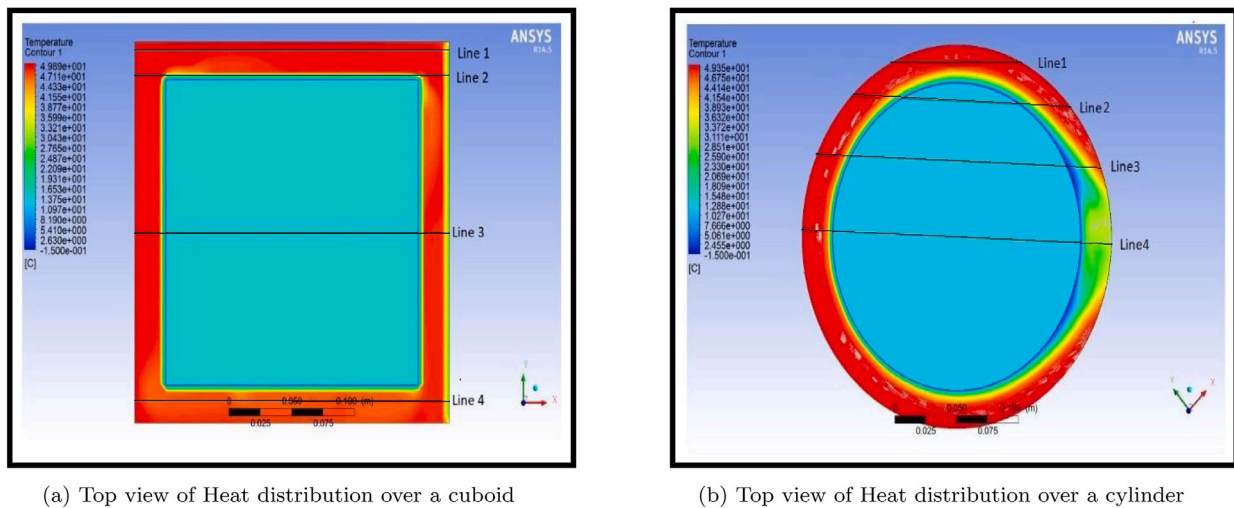
Fig. 3. Heat transfer analysis across design geometries.

(a) Graphical representation of the heat flow over cuboid

(b) Graphical representation of the heat flow over cylinder
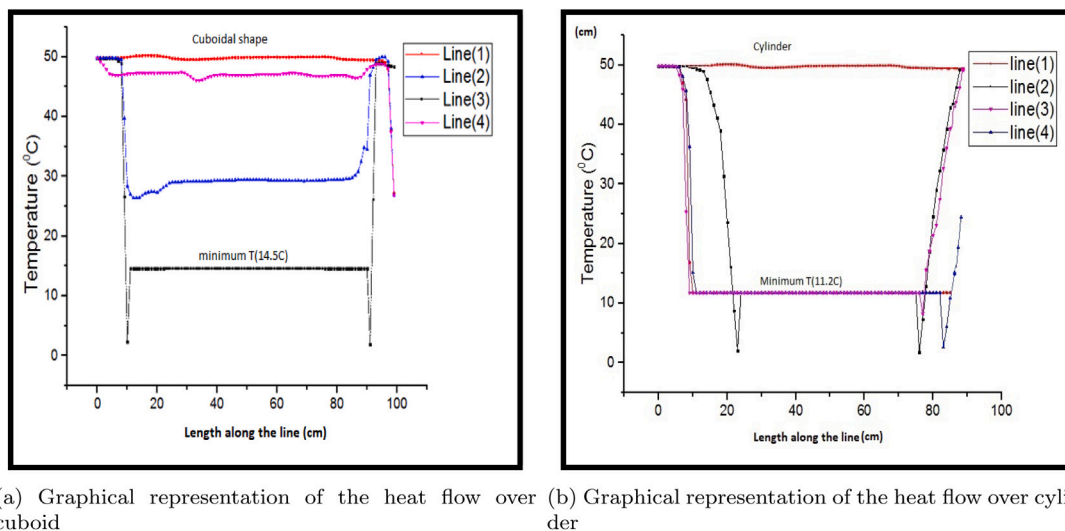
Fig. 4. Graphical heat transfer plots over 4 cross sectional planes over the geometries.

(a) Power vs Temp Curve for all tested PCMs

(b) Calculated Area under the Curve for 1-Decanol

Fig. 5. DSC curves for analysis.

(a) Different parts and Compartments of the Tray

(b) Mesh for simplified geometry of Tray Assembly
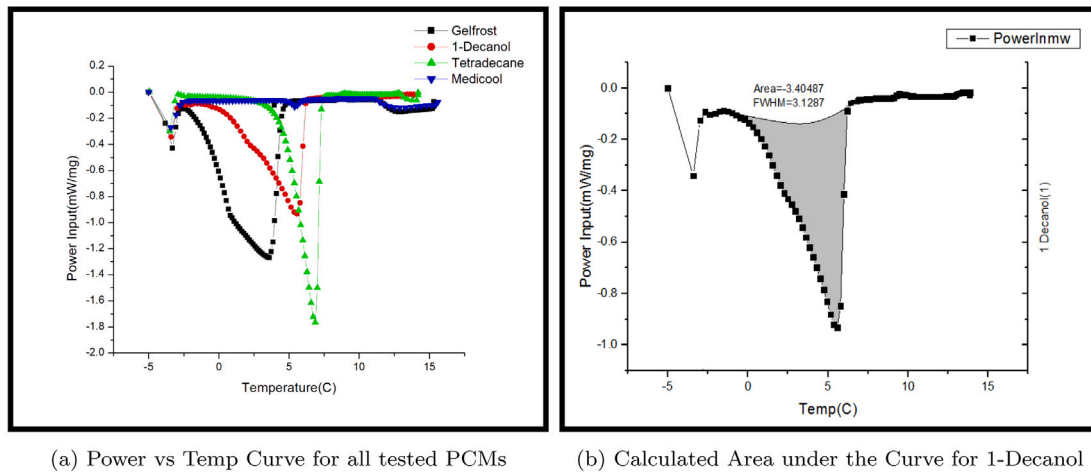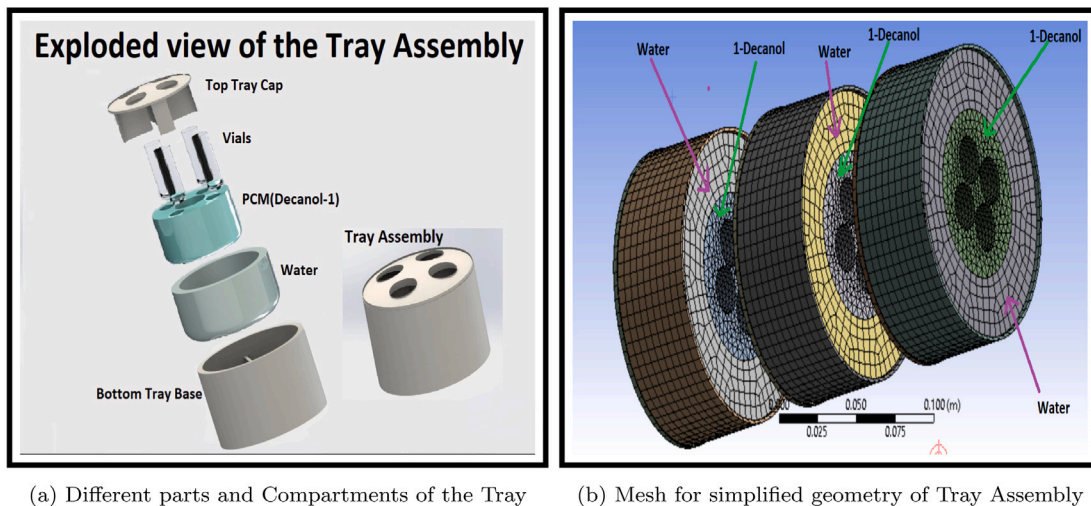
Fig. 6. Tray design assembly.

two PCMs has the potential to offer greater resistance to heat over a wider range in the critical temperature limits of the vaccines 2–8 °C.

With the proposed new design and simulation philosophy as highlighted in Section 2.1.2, a conjugate heat transfer analysis is performed using Eqs. (1),(2) & (3) along the boundary conditions as given in Table 5. The significant difference from boundary conditions applied on the original design(Table 4) is that an ambient temperature of 26° C is applied. This temperature is chosen as it is a reasonable average ambient temperature that the vaccine carrier could be exposed to, but more consequentially it is a temperature that is closer to the one that can be consistently maintained during the experimental evaluation of the new design. This would aid the direct comparison of the results from the simulation with the experimental results. Most of the material of construction is chosen to be the same as the original design; thus, the same material properties are applied(See Appendix O). However, since the proposed vaccine tray is a novel feature in the new design, the simulation is used to narrow down some key properties for MOC of the tray via successive trials in the boundary conditions, particularly the Thermal Conductivity(K). The final thermal conductivity of 0.3 Wm/K as presented in Table 5 is arrived at post several modifications, reruns and adjustments until the results serve purpose of the design process.

3.4.1. Application of UDF

In order to capture the thermo-physical features of the PCM based vaccine assembly, a set of adjustment to the ambient temperature

Table 5

Constraints applied along critical properties on the new design.

Parameter	Boundary Conditions
Outside ambient temperature	T = 26 °C, This is applied along the UDF {see Appendix G}
Inside vaccine space temperature	T = 6 °C
Tray temperature	T = 0 °C
Convective heat transfer of air coefficient(Outside)	h = 4 W/(m² K) @ T = 26 °C
Convective heat transfer of air coefficient(inside)	h = 1 W/(m² K) @ T = 6 °C
Latent heat of PCM(Water)	$\lambda 1$ = 323 kJ/(kg)
Latent heat of PCM(1-Decanol)	$\lambda 2$ = 270 kJ/(kg)
Thermal conductivity of trays	K = 0.3 W m/K

boundary conditions at the lid is applied. For this, a UDF(User Defined Function) written in C language is implemented to define variable heat flux across the height of the assembly. The focus is to periodically 'plug' the outside ambient temperature from the top over a 14-second cycle as shown in Fig. 7. This is done with the intent to replicate realistic usage as explained in Section 2.2 and the effect of opening the top lip of the
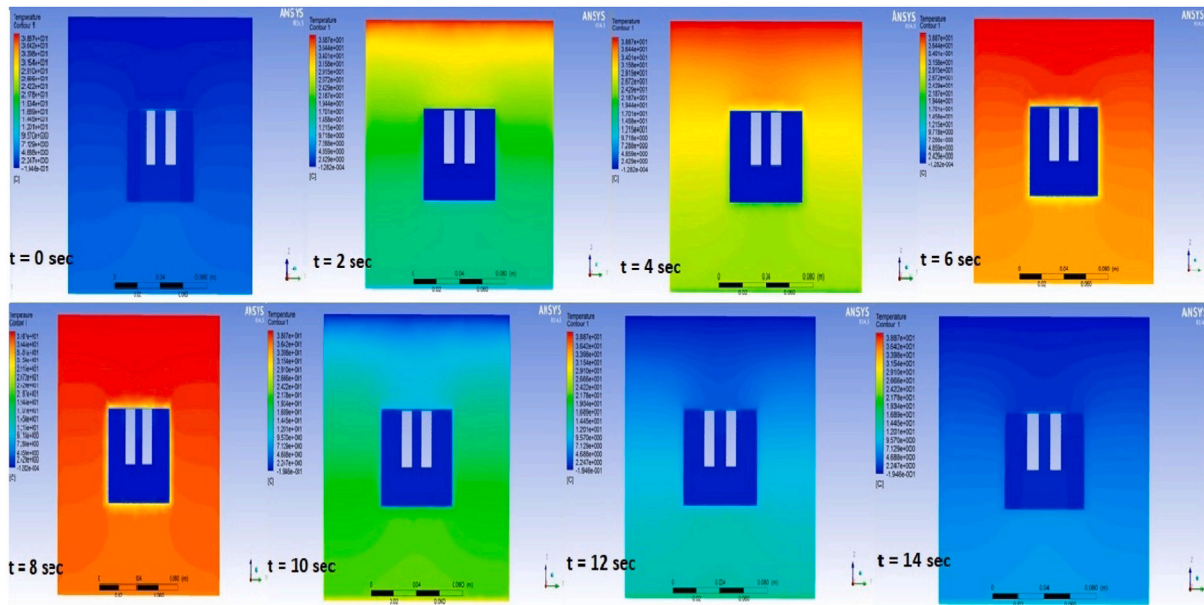
Fig. 7. Cross-sectional contours presenting transient state simulations for Thermal Exposure of Tray due to the UDF applied over a 14 s cycle

assembly to take out a vaccine vial [30]. As depicted in Fig. 7, the lid is closed at t = 0 s and the opening is initiated until till it is closed again at t = 14 s, interim which the contours(at t = 2, 4, 6, 8, 10, 12 s) present the immediate thermal distribution when exposed directly to ambient temperatures.

3.4.2. Results for the tray assembly

The results obtained in Fig. 8 show the contours obtained for a 45 h transient analysis with UDF boundary condition applied (Fig. 7) at every theoretical hour of the simulated timescale. Results shown in Fig. 8 are indicative that such a system can minimize temperature gradients along the height of the assembly which otherwise develop through convection of air within the storage space. Such a tray system has PCMs with simultaneous melting within the range of 0–6 °C that show reduced differential temperatures by creating thermal subsystem at various level within them.

The simulation results suggest that a suitable internally cooled environment can be sustained for 45 h which is much higher than for original design. However, this is expected to be an overestimation since simplified geometry 6(b) & various assumptions are made as per Section 2.1.2. Although the potential for such a design shows evident promise in its application, it offers enhanced utility by limiting the thermal exposure to the top tray in use when the lid is opened protecting the trays kept underneath. Also, sufficient protection for the base provided by such a system is critical since the results on the original design (Section 3.1) show that significant heat penetration from the base [7,15,32].

3.5. Results regarding MOC selection for the tray

As per the selection criteria mentioned in Section 2.3 and the results from Section 3.4.2 show that in order to effectively insulate the vials from the atmospheric temperatures and also allow heat flow from the vials, the thermal conductivity is kept as 0.3 W/mk. Thus, the applied constraints as shown in Table 2 are kept within the range of 0.1–0.7 W/mK.

From this process, four possible materials(from Figs. 9(a) & 9(b)) for the vaccine tray are chosen based on the constraints. The materials are Polyethylene-Low Density(PE-LD), Polyethylene Terephthalate (PET with 45% glass fibre), Polybutylene (PB), Polypropylene (PP) and PP (with 50% long glass fibre). Based on this data, a selection

matrix(details given in Appendix F) is created to rate the candidates and select the most suitable one. From this analysis, PP is chosen as the final MOC of the tray and used to prepare a 3-D printed prototype as depicted in Figs. 10(a) & 10(b). The polymer filament is purchased from Ultimaker and 0.4 mm nozzle size on Creatbot DX fused deposition Printer is utilized.

3.6. Experimental evaluation

The new design incorporates three PCM encapsulated trays lined in a vertical assembly inside an overall cylindrical design. Similar material features as the original design are incorporated in this design; the core insulation is provided by a cylindrical 45 mm thick lining of Polyurethane. The outer lining has HDPE coating while the inner lining has a Polystyrene lining. Each tray, designed to be a replacement for the conventional coolant packs in the original design, is loaded with 150 g of 1 Decanol and 200 g of water. The tray holds about 350 g of PCM within and three such trays weigh about 1250 g cumulatively. Besides this, another 50 mm thick polyurethane layer forms the insulation at the bottom.

As per the assembly details presented in Fig. 11(a), hing joint clips are added to hold three trays stacked vertically. Similarly, Fig. 11(b) provides detailed design drafts of the overall vaccine carrier outer casing along which a cylindrical design of 20 cm height with 10 cm radius is fabricated, a 45 mm polyurethane layer defines the insulated core. The fabricated new design is tested with the setup to monitor inside temperature and evaluate R-value as described in Section 2.4 with one distinction that 6 temperature sensors are used instead of 7(Like in the case for original design). The schematic diagram(Fig. 12(a)) of the setup describes the relative positioning of the temperature sensors and non-metallic box for the melt test with two level indicators & two Aluminium foils. The overall assembly to test the new design is given in Fig. 12(b).

The corresponding results obtained for the experimental setup (Fig. 12(b)) is depicted in Figs. 13 & 14. The Figs. 13(a), 13(b) portray the temperature profile for T_1/T_2 and T_3/T_4 wall sensors which lie near the lower and upper ends from the bottom of the new design, respectively. The profiles, in general, show a semi-consistent trend to the simulation curve developed from the earlier Section 3.4. There are two significant horizontally parallel or 'flat' regions that account for phase change behaviour of water and 1-Decanol near about 0 °C &
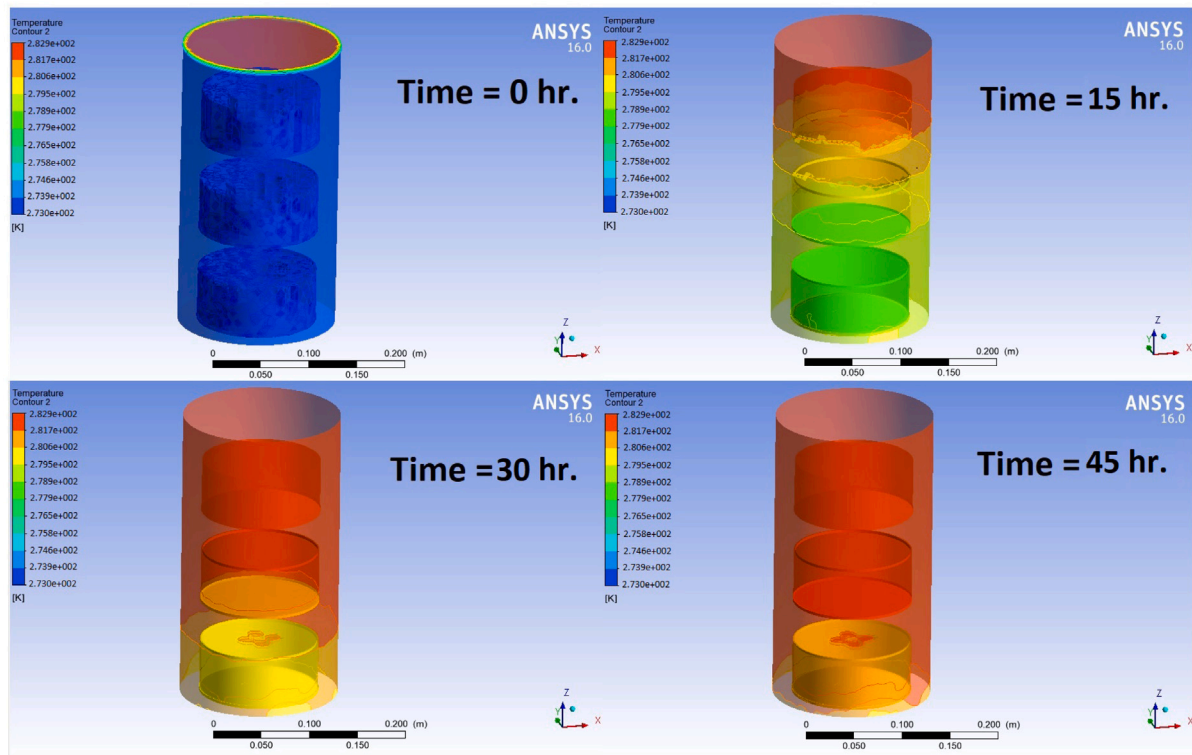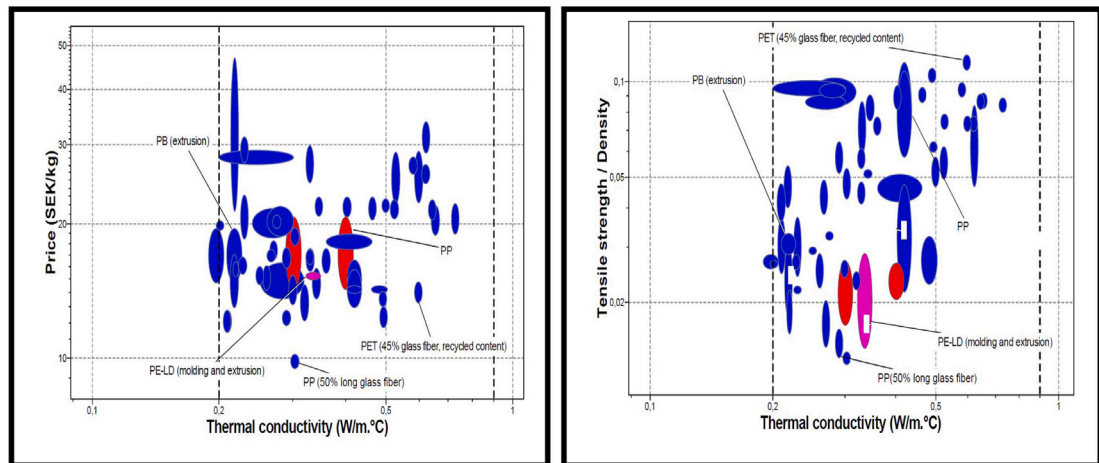
Fig. 8. Depiction of the 45 h transient analysis of the Tray system with the applied 14 s cyclic UDF boundary condition.

(a) Price per Kg vs Thermal Conductivity

(b) Tensile Strength/Density vs Thermal Conductivity

Fig. 9. Ashby plots for material selection.

6 °C, respectively. The physics of these flat zones near 6 °C is confirmed with a similar distribution of experimental data points in 13(a) & 13(b). However, the simulated flat curvature near 0°C is not entirely reflected in the corresponding thermal data points. The reason for this could be an apparently higher rate of temperature increase in water, which is 'conditioned' just like for a conventional design as mentioned in Section 1 and [39]. Besides, significant consistent overshoot in the experimental temperature at a given time from the simulated data is an obvious outcome owed to the assumptions and modifications made for the simulation.

Fig. 14(a) showcases the profile for T_5 sensor placed at the top of the non-metallic box such that it is in very close proximity to the bottom tray and melting ice cube inside the non-metallic box. Consequently, more prominent flat zones are observed near 0 °C & 5 °C for the

simulation, which are not equally matched by the experimental values. The experimental profile of the bottom-most sensor has significant flat zones in 0 °C but not a significant one at 5 °C as the non-metallic box placed has 100 g of ice but no 1-Decanol. The experimental readings from T_5 sensor show much higher temperature readings which surpass the upper threshold 1(8 °C) at the 27 h mark. A moving average for all the six sensors is applied and the average time to surpass the upper threshold 1(8 °C) mark for the system is calculated to be 30.2 hrs. The simulation profiles on an average show about 21% deviation from experimental values, with the higher end of deviation, found for T_5 and T_6 sensor. This consistent deviation observed can be attributed to the limitation in fully simulating the multi-modal transmission of heat in the actual system, specifically the effect of radiation heat transfer from opening the assembly which is assumed to be zero for this model.
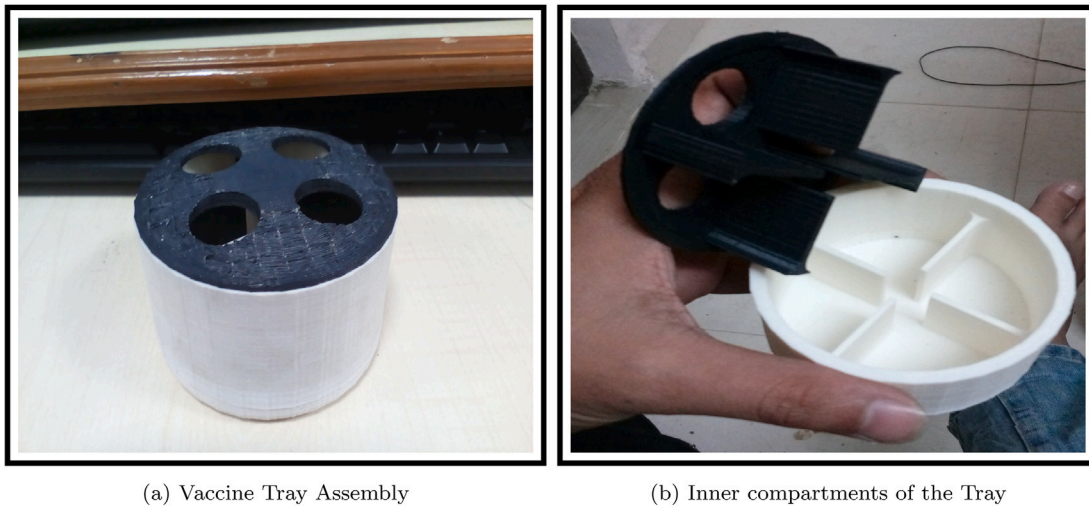
(a) Vaccine Tray Assembly

(b) Inner compartments of the Tray

Fig. 10. Proposed vaccine tray for the new design.

(a) Vaccine Tray stacking system
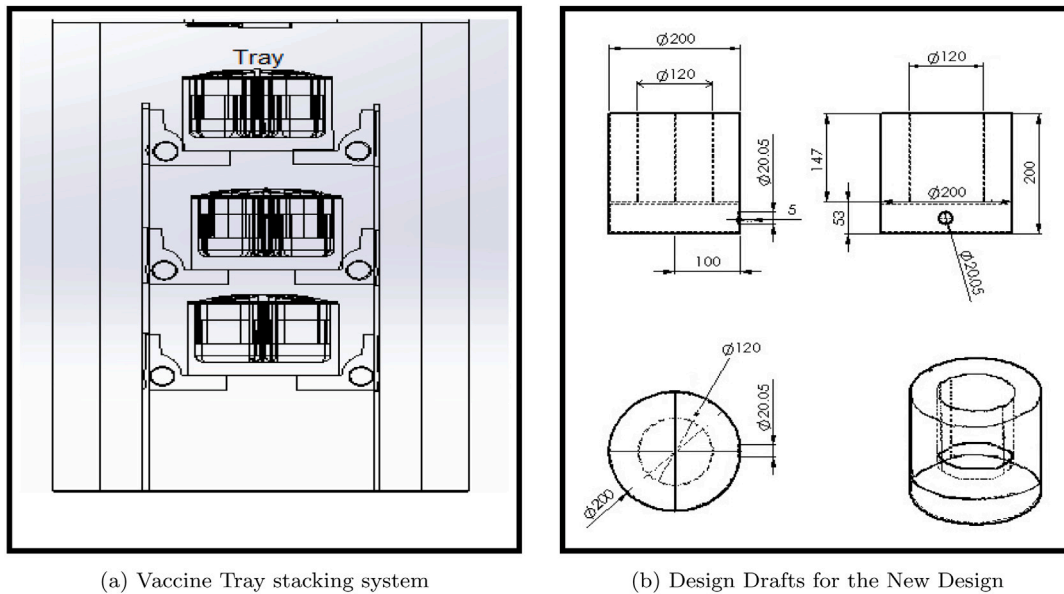

(b) Design Drafts for the New Design

Fig. 11. Details for the new design.

Also the significant effect of conductive heat transfer from the bottom as identified from analysis of original design in Section 3.1) and its effect along with radiation is largely under-computed in the simulation. Also larger inconsistencies is also due to the fact that the simulated model is set at 26 °C ambient temperature while a consistent ambient temperature of only 24 °C could be practically maintained throughout the duration of experiment. Although this is the key reason for this divergence, the conjugate heat transfer modelling is still not accounting a significant radioactive component of heat transfer physics involved here. However, in the broader context of this exercise the generic trends of phase change could still be compared to arrive at significant insight into understanding the phenomenon. These factors are indicative of broad scope in improving the simulation model to represent the physics of the assembly in detail.

Besides the 30.2 h average vaccine potency time, another significant outcome recorded from the experiment is the melt time of 15.2 h for 100 g. Using Eqs. (5)&(6) from Section 2.4, the following are obtained,

$$\text{Melt Rate } = \frac{\text{Mass of ice cube}}{\text{Melting time}} = \frac{0.1 \text{ kg}}{15.2 \text{ hr.}} = 0.00658 \text{ kg/hr} \quad (8)$$

Using Eq. (5) and plugging in values for the inside area of the design as 0.135 m², the temperature difference between ambient and inside temperature as 24 °C, latent heat of vaporization as 323 kJ/kg and melting rate from (8),

$$\text{System R-Value } = \frac{(0.135 \text{ m}^2)(24 \text{ °C} - 0 \text{ °C})}{(0.00658 \text{ kg/hr})(323 \text{ kJ/kg})} = 5.489 \text{ (m}^2.\text{°C)/W} \quad (9)$$

Using Eq. (6) and plugging in values from the average wall thickness of 10 cm, 6 being the number of individual interior walls that forms the cylindrical inside lining and 2 aluminium foils added to the non-metallic box.

$$5.489 \cong 0.27(10) + 0.26(6) + 0.56(2) \quad (10)$$

$$5.489 \cong \underbrace{2.7}_{C} + \underbrace{1.56}_{c} + \underbrace{1.12}_{R} \; (\approx -2\%error) \quad (11)$$
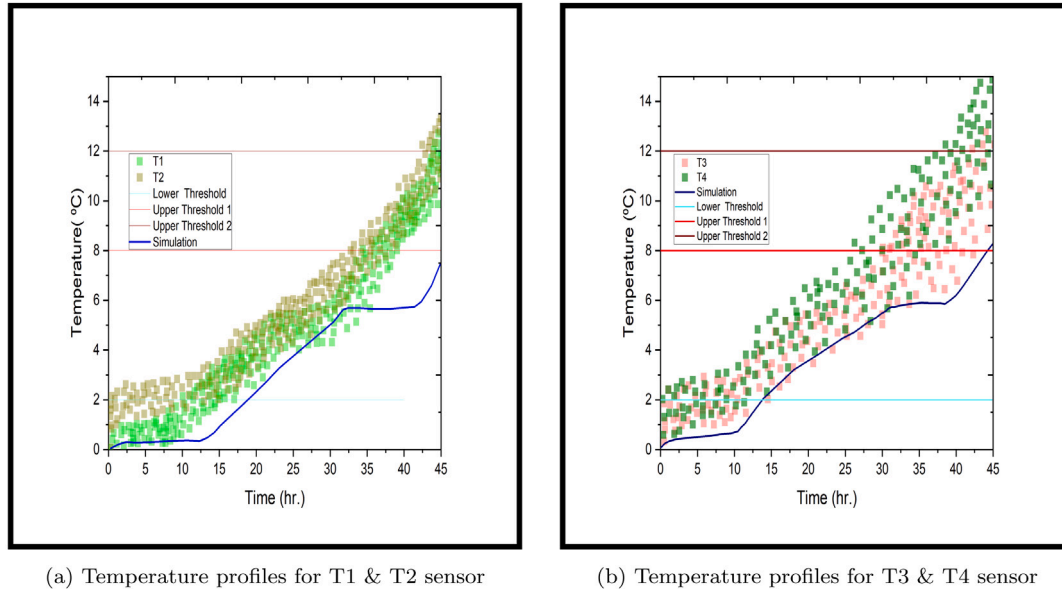
$$= 49.19 \text{ \%}(Conduction) + 28.42 \text{ \%}(Convection) + 20.40 \text{ \%}(Radiation) \quad (12)$$

The above section provides the final outcome of this exercise in which an R-value of 5.489 m² °C/W for the new design is obtained, alongside which the total penetration of heat into the new design assembly is
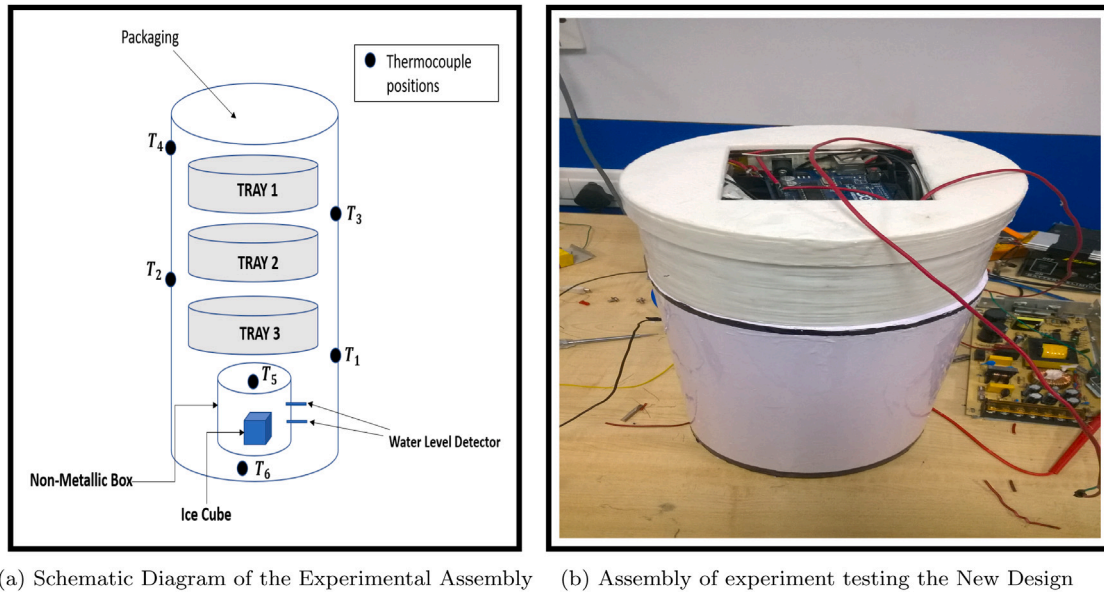
(a) Schematic Diagram of the Experimental Assembly

(b) Assembly of experiment testing the New Design

Fig. 12. Temperature profiles for sensors as compared with the simulation profile at the corresponding plane.

(a) Temperature profiles for T1 & T2 sensor

(b) Temperature profiles for T3 & T4 sensor

Fig. 13. Experimental and simulation profile of 4 wall temperature sensors.

attributed to 49.19% conduction, 28.42% convection, 20.40% radiation as per the obtained value.

4. Discussion

A systematic approach for improving the original or conventional vaccine carrier box by introducing similar design features of products such as [23–26] has been devised and tested to showcase its quantitative impact on insulation performance. The design approach begins with understanding the engineering and underlying heat transfer physics for the original design; its insulation capacity is examined by R-value test, monitoring temperature profiles within the box and conjugate heat transfer modelling. Actual results drawn from this is that the continuous and prolonged contact of the base with the ground leads to the dominant role of conductive heat transfer from the bottom followed by the development of thermal gradients along the vertical axis or height of the assembly. For the new design, a series of steps

taken are geometry modelling, heat transfer simulation, MOC & PCM characterization, fabrication. This is followed by testing corresponding temperature profiles within & evaluating the R-value for the new design. The essential core for the new design is its cylindrical design inside which a stacked vaccine tray assembly is devised to wear off the emergence of thermal gradients along the height of the carrier.

One of the major factors considered when designing and fabricating the new design is to replicate original design's volume and size scales along with the identical MOCs for the outer casing. This is done to maintain a consistent comparison of performance across similar scales for the vaccine carrier box. The results from Table 6 present a comparison across several parameters relevant to this study.

The most prominent result from Table 6 is the 17.05% improvement in average vaccine safekeeping time in the 2–8 °C range for the new design. Another significant increase of about 2 h in the ice cube melt time is consequently reflected in the final R-value obtained. Its 16.19% increment is a reflection of the improved insulation capability offered
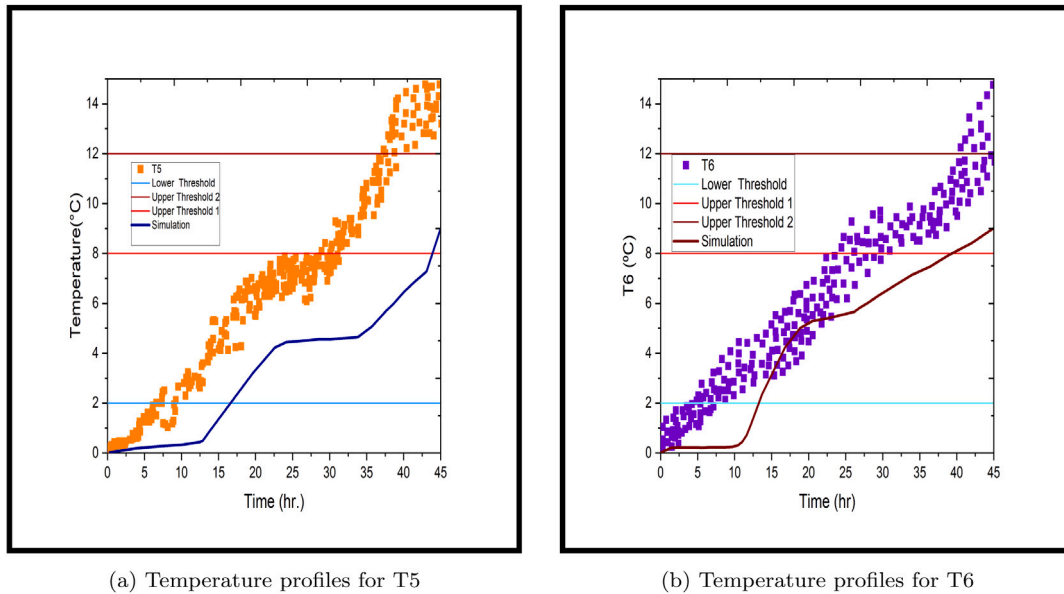
(a) Temperature profiles for T5

(b) Temperature profiles for T6

Fig. 14. Experimental and simulation profile of the 2 bottom temperature sensors.

Table 6
Comparison of the original and new design.

Parameter	Original design	New design
Shape	Cubical	Cylindrical
Principle passive cooler	4 Coolant packs	3 Vaccine trays
Inside area	0.14 m^2	0.135 m^2
Average vaccine safe keeping time	25.8 h	30.2 hr(17.05% ↑)
100 g ice-cube melting time	13.02 h	15.2 h
Principle PCM employed	Water	Water & 1-Decanol
R-value (m^2 °C/W)	4.724	5.489(16.19% ↑)
Conduction contribution	51.43%	49.19%
Convection contribution	27.51%	28.42%
Radiation contribution	23.7%	20.40%

by the features of the new design. Such features are essentially its cylindrical design, vaccine tray stacked assembly and the two PCMs employed within each tray. The two PCMs namely Water and 1-Decanol, as theorized offer sacrificial melting in the temperature ranges of 0–4 °C and 4–6 °C, respectively. It leads to an increase in melting time and R-value; however, a potential shortcoming of this analysis is its inability to isolate the effects of the two described features of the new design. Thus, the effect of individual features on the insulation capability of the new design is ambiguous and cannot be quantified within the scope of the experimental work presented here. However, it is quite evident that the cumulative effect of these features provides the basis for a potentially superior design. Another outcome from Table 6 are the largely unchanged contributions of each mode of heat transfer which is a reflection of the similar scales of the two tested designs and principle of operation relying on identical MOCs. The slight variations in the percentage numbers for conduction, convection, radiation can be attributed to the $\pm20\%error$ range in the empirical formula used (Eq. (6)), this is also the reason for their summation not leading to a perfect 100%. Besides, the effect of this is not entirely captured by the conjugate heat transfer model, as discussed in Section 2.4. Another observation from Table 6 is that the original design packs 4 coolants whereas the new design only 3, which limits its vaccine and PCM carrying capacity. However, the removal of the non-metallic box at the bottom, which was a requirement for this experiment, could improve upon the number of vaccine/PCM Tray that could be carried by this design for regular usage.

Another vital advantage provided by the new design is that due to the placement and distribution of PCM encapsulated trays stacked
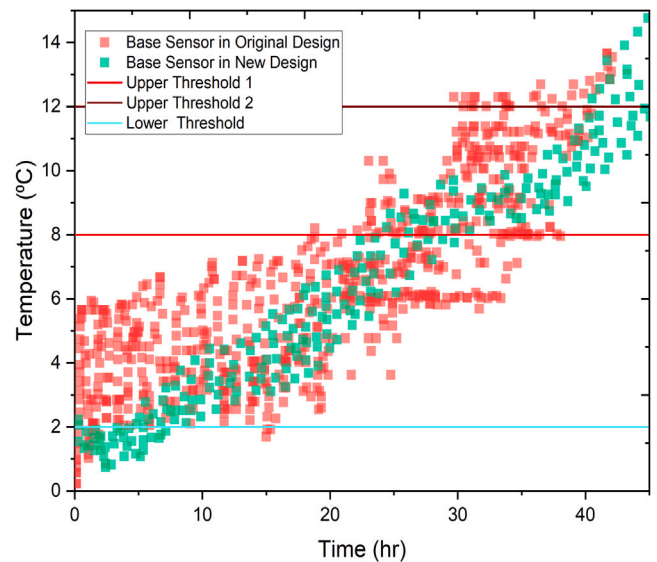

Fig. 15. Comparison of ground sensors for the 2 designs.

in the form of vertical assembly, development of differential thermal gradients along the height of the vaccine carrier are widely suppressed when compared to the original design. One of the major factors considered when designing and fabricating the new design is to replicate the original design's volume and size scales along with the identical MOCs for the outer casing to maintain a consistent comparison of performance across similar scales for the vaccine carrier box. The wide temperature fluctuations is observed across all temperature sensors in Fig. 2(a) for the original design. Such fluctuations are significantly reduced consistently for each positional sensor as seen from Figs. 13 & 14 when compared to there counterparts in the original design (Fig. 2(a)). Fig. 15 summarizes this observation, the base sensor for the original design showed the most fluctuations due to conductive heat transfer from the bottom of the vaccine carrier which is evident from the varied range of temperatures reported within a short interval of time. When a refined moving average is applied over the readings from Fig. 15, a ~ 22% increased time to cross the upper threshold 1(8 °C)

for the new design(∼ 26 h) is noted when compared to the original design(∼ 20.3 h). Another important observation is that the temperature values obtained are across a narrower range for the new design when compared to the original design. This reiterates that the new design suppresses the temperature fluctuations and limits the development of thermal gradients.

5. Conclusion

The work adapts quantification approaches to mark out the effect on insulation performance of the Original (conventional) vaccine carrier box by modifications to make a cylindrically aligned New Design which efficiently utilizes the central vaccine storage space via a vertically stacked tray assembly. A 17% improved performance in terms of vaccine safekeeping time is obtained with 16.19% improvement in the measured R-value for the new design. This overall increase in the insulation performance of the new design is indicative of the superior performance(as high as 72 h) reported by some of the commercial designs [23–26] which share similar design features but also possess advanced integrated active cooling systems. Although the entry of these semi-passive/passive cooling products has been restrictive to lower& middle-income hot climate countries, more designs are being developed and put to clinical Trial stage. The study here presents a comprehensive engineering approach as a useful backdrop to further develop a more appropriate vaccine cold chain carrier for rural delivery.

CRediT authorship contribution statement

Shitanshu Devrani: Conceptualization, Methodology, Software, Data curation, Formal analysis, Investigation, Validation, Visualization, Writing - original draft, Writing - review & editing. **Rahul Tiwari:** Conceptualization, Methodology, Software, Data curation, Formal analysis, Investigation, Validation. **Naseef Khan:** Conceptualization, Methodology, Software, Data curation, Formal analysis, Investigation, Validation, Visualization. **Krishnakumar Sankar:** Methodology, Software, Data curation, Formal Analysis, Investigation, Validation, Visualization. **Shantanu Patil:** Methodology, Data curation, Project administration, Resources. **K. Sridhar:** Data curation, Project administration, Resources, Funding acquisition.

Declaration of competing interest

There are no competing conflicts of interest. The funding for the Project was provided by SRM Medical College Hospital & Research Centre, (603203), Kattankulathur, India.

Acknowledgements

The authors gratefully acknowledge the funding received from SRM Medical College Hospital and Research Centre (SRM MCHRC) and also the Department of Community Medicine for valuable feedback.

Appendix A. Supplementary data

Supplementary material related to this article can be found online at https://doi.org/10.1016/j.est.2020.102182.

References

[1] D.M. Matthias, J. Robertson, M.M. Garrison, S. Newland, C. Nelson, Freezing temperatures in the vaccine cold chain: A systematic literature review, Vaccine 25 (20) (2007) 3980–3986, http://dx.doi.org/10.1016/j.vaccine.2007.02.052, https://linkinghub.elsevier.com/retrieve/pii/S0264410X07002289.

[2] B. McCormick, D. Koenig, The R-value of global health (conserving energy to save lives), in: 2010 Annual International Conference of the IEEE Engineering in Medicine and Biology, IEEE, Buenos Aires, 2010, pp. 1104–1107, http://dx.doi.org/10.1109/IEMBS.2010.5627363, http://ieeexplore.ieee.org/document/5627363/.

[3] E. Rosenthal, The price of prevention: Vaccine costs are soaring, N.Y. Times (2014) https://www.nytimes.com/2014/07/03/health/Vaccine-Costs-Soaring-Paying-Till-It-Hurts.html.

[4] T. Wirkas, S. Toikilik, N. Miller, C. Morgan, C.J. Clements, A vaccine cold chain freezing study in PNG highlights technology needs for hot climate countries, Vaccine 25 (4) (2007) 691–697, http://dx.doi.org/10.1016/j.vaccine.2006.08.028, https://linkinghub.elsevier.com/retrieve/pii/S0264410X06009601.

[5] C.A. Boros, M. Hanlon, M. Gold, D. Roberton, Storage at −3° C for 24 h alters the immunogenicity of pertussis vaccines, Vaccine 19 (25) (2001) 3537–3542, http://dx.doi.org/10.1016/S0264-410X(01)00063-9, http://www.sciencedirect.com/science/article/pii/S0264410X01000639.

[6] Centers for Disease Control and Prevention, Vaccine storage and handling guidelines, Fact Sheet (2018) 24, https://www.cdc.gov/vaccines/hcp/admin/storage/index.html.

[7] Spoerke, et al., Thinking Outside the (cool) Box, Georgia Institute of Technology, 2010, http://www.colton.gatech.edu/detm/coolboxfinalreport.pdf.

[8] S.-I. Chen, B.A. Norman, J. Rajgopal, B.Y. Lee, Passive cold devices for vaccine supply chains, Ann. Oper. Res. 230 (1) (2015) 87–104, http://dx.doi.org/10.1007/s10479-013-1502-5.

[9] C.L. Karp, D. Lans, J. Esparza, E.B. Edson, K.E. Owen, C.B. Wilson, P.M. Heaton, O.S. Levine, R. Rao, Evaluating the value proposition for improving vaccine thermostability to increase vaccine impact in low and middle-income countries, Vaccine 33 (30) (2015) 3471–3479, http://dx.doi.org/10.1016/j.vaccine.2015.05.071, https://linkinghub.elsevier.com/retrieve/pii/S0264410X15007446.

[10] U. Kartoglu, J. Milstien, Tools and approaches to ensure quality of vaccines throughout the cold chain, Expert. Rev. Vaccines 13 (7) (2014) 843–854, http://dx.doi.org/10.1586/14760584.2014.923761, http://www.tandfonline.com/doi/full/10.1586/14760584.2014.923761.

[11] R.P. Beasley, Rocks along the road to the control of HBV and HCC, Ann. Epidemiology 19 (4) (2009) 231–234, http://dx.doi.org/10.1016/j.annepidem.2009.01.017, https://linkinghub.elsevier.com/retrieve/pii/S1047279709000489.

[12] D. Chen, D. Kristensen, Opportunities and challenges of developing thermostable vaccines, Expert. Rev. Vaccines 8 (5) (2009) 547–557, http://dx.doi.org/10.1586/erv.09.20, http://www.tandfonline.com/doi/full/10.1586/erv.09.20.

[13] D.D. Kristensen, T. Lorenson, K. Bartholomew, S. Villadiego, Can thermostable vaccines help address cold-chain challenges? Results from stakeholder interviews in six low- and middle-income countries, Vaccine 34 (7) (2016) 899–904, http://dx.doi.org/10.1016/j.vaccine.2016.01.001, Edition: 2016/01/08 Publisher: Elsevier Science, https://pubmed.ncbi.nlm.nih.gov/26778422.

[14] WHO, Global vaccine market report, Mark. Inf. Access Vaccines (2019) https://www.who.int/immunization/programmes_systems/procurement/mi4a/platform/module2/2019_Global_Vaccine_Market_Report.pdf?ua=1.

[15] Conway, et al., Improving Cold Chain Technologies Through the Use of Phase Change Material, Gemstone Program, University of Maryland, 2012, p. 227, https://drum.lib.umd.edu/bitstream/handle/1903/12491/FRESH.pdf;jsessionid=5B40C43AC0BFB10B3F3BF4C17BA85B23?sequence=1.

[16] A. container Package System Sweden A.B., et al., Cool Innovations for Vaccine Transportation and Storage, Report, 2012, https://www.who.int/immunization/programmes_systems/supply_chain/optimize/Cooling_17july12.pdf.

[17] Y. Zhao, X. Zhang, X. Xu, S. Zhang, Development of composite phase change cold storage material and its application in vaccine cold storage equipment, J. Energy Storage 30 (2020) 101455, http://dx.doi.org/10.1016/j.est.2020.101455, https://linkinghub.elsevier.com/retrieve/pii/S2352152X20304564.

[18] N. Putra, Design, manufacturing and testing of a portable vaccine carrier box employing thermoelectric module and heat pipe, J. Med. Eng. Technol. 33 (3) (2009) 232–237, http://dx.doi.org/10.1080/03091900802454517, http://www.tandfonline.com/doi/full/10.1080/03091900802454517.

[19] S. Chatterjee, K. Pandey, Thermoelectric cold-chain chests for storing/transporting vaccines in remote regions, Appl. Energy 76 (4) (2003) 415–433, http://dx.doi.org/10.1016/S0306-2619(03)00007-2, https://linkinghub.elsevier.com/retrieve/pii/S0306261903000072.

[20] E. Reid, J. Barkes, C. Morrison, A. Ung, R. Patel, C. Rebarker, P. Panchal, S. Vasa, Design and Testing of a Thermoelectrically-Cooled Portable Vaccine Cooler, Tech. rep., Journal of Young Investigators, 2018, http://dx.doi.org/10.22186/jyi.35.2.50-55, https://www.jyi.org/2018-august/2018/7/30/design-and-testing-of-a-thermoelectrically-cooled-portable-vaccine-cooler.

[21] P.H. Pedersen, J. Maté, Solarchill vaccine cooler and refrigerator: a breakthrough technology, in: Interlinked Challenges, Interlinked Solutions: Ozone Protection and Climate Change, Citeseer, 2006, p. 17, http://citeseerx.ist.psu.edu/viewdoc/download?doi=10.1.1.120.3614&rep=rep1&type=pdf#page=17.

[22] E. Elsarrag, O.N. Igobo, Y. Alhorr, P.A. Davies, Solar pond powered liquid desiccant evaporative cooling, Renew. Sustain. Energy Rev. 58 (2016) 124–140, http://dx.doi.org/10.1016/j.rser.2015.12.053, https://linkinghub.elsevier.com/retrieve/pii/S1364032115014367.

[23] Bloedow, et al., (54) Temperature-stabilized storage systemis with regulated cooling, 2013, US Patent, https://patents.google.com/patent/WO2014194022A1/en.

[24] Novisoff, et al., Mobile thermoelectric vaccine cooler with a planar heat pipe, 2015, US Patents, https://patents.google.com/patent/US20160003503A1/en.

[25] O.T. NEPI, Unplugged and keeping cool—Testing off-grid vaccine storage solutions in Vietnam, 2013, PATH-WHO, http://iaphl.org/wp-content/uploads/2016/05/Testing-off-grid-vaccine-storage-solutions-in-Vietnam.pdf.

[26] T. Grandry, et al., Renowned medical devices Colli-Pee and Cool-VAX at design exhibit, Novosanis (2016) https://novosanis.com/news/renowned-medical-devices-colli-pee-and-cool-vax-design-exhibit.

[27] Passive Vaccine Storage Device (PVSD), Cold Chain IQ BM Report, Cold Chain IQ Benchmarking Report 2014, 2013, p. 2, https://www.pharmalogisticsiq.com/supply-chain-security-track-trace/whitepapers/cold-chain-iq-benchmarking-report-7-best-practice.

[28] S.T. Brown, B. Schreiber, B.E. Cakouros, A.R. Wateska, H.M. Dicko, D.L. Connor, P. Jaillard, M. Mvundura, B.A. Norman, C. Levin, J. Rajgopal, M. Avella, C. Lebrun, E. Claypool, P. Paul, B.Y. Lee, The benefits of redesigning Benin's vaccine supply chain, Vaccine 32 (32) (2014) 4097–4103, http://dx.doi.org/10.1016/j.vaccine.2014.04.090, https://linkinghub.elsevier.com/retrieve/pii/S0264410X14006410.

[29] J. Lloyd, S. McCarney, R. Ouhichi, P. Lydon, M. Zaffran, Optimizing energy for a 'green' vaccine supply chain, Vaccine 33 (7) (2015) 908–913, http://dx.doi.org/10.1016/j.vaccine.2014.10.053, https://linkinghub.elsevier.com/retrieve/pii/S0264410X14014431.

[30] Széchenyi István University, P. Böröcz, A. Mojzes, Széchenyi István University, P. Csavajda, Measuring and analysing the effect of openings and vibration on reusable pharmaceutical insulated boxes with daily distribution, J. Appl. Packag. Res. 7 (2) (2015) 32–44, http://dx.doi.org/10.14448/japr.04.0002, http://scholarworks.rit.edu/japr/vol7/iss2/2/.

[31] S. Akdemir, Evaluation of cold storage insulation by thermal images analysis, Bulg. J. Agric. Sci. 20 (2014) 246–254, https://www.agrojournal.org/20/02-04.pdf.

[32] S. Devrani, S. Pandey, S. Chaturvedi, K. Sankar, S. Patil, K. Sridhar, Design and analysis of an efficient vaccine cold chain box, in: Volume 3: Biomedical and Biotechnology Engineering, American Society of Mechanical Engineers, Phoenix, Arizona, USA, 2016, http://dx.doi.org/10.1115/IMECE2016-65858, V003T04A018, https://asmedigitalcollection.asme.org/IMECE/proceedings/IMECE2016/50534/Phoenix,%20Arizona,%20USA/257141.

[33] K. Wang, L. Yang, M. Kucharek, Investigation of the effect of thermal insulation materials on packaging performance, Packag. Technol. Sci. 33 (6) (2020) 227–236, http://dx.doi.org/10.1002/pts.2500, https://onlinelibrary.wiley.com/doi/abs/10.1002/pts.2500.

[34] G. Burgess, Practical thermal resistance and ice requirement calculations for insulating packages, Packag. Technol. Sci. (1999) 6, https://onlinelibrary.wiley.com/doi/epdf/10.1002/%28SICI%291099-1522%28199903/04%2912%3A2%3C75%3A%3AAID-PTS454%3E3.0.CO%3B2-2.

[35] M. Kucharek, L. Yang, K. Wang, Assessment of insulating package performance by mathematical modelling, Packag. Technol. Sci. 33 (2) (2020) 65–73, http://dx.doi.org/10.1002/pts.2492, https://onlinelibrary.wiley.com/doi/abs/10.1002/pts.2492.

[36] H. Lundbeck, B. Håkansson, J.S. Lloyd, S.K. Litvinov, F. Assaad, A cold box for the transport and storage of vaccines, Bull. World Health Organ. 56 (3) (1978) 427–432, https://www.ncbi.nlm.nih.gov/pmc/articles/PMC2395592/pdf/bullwho00440-0097.pdf.

[37] R. Ravotti, O. Fellmann, L.J. Fischer, J. Worlitschek, A. Stamatiou, Investigation of the thermal properties of diesters from methanol, 1-pentanol, and 1-decanol as sustainable phase change materials, Materials 13 (4) (2020) 810, http://dx.doi.org/10.3390/ma13040810, https://www.mdpi.com/1996-1944/13/4/810.

[38] R. Ravotti, O. Fellmann, N. Lardon, L. Fischer, A. Stamatiou, J. Worlitschek, Synthesis and investigation of thermal properties of highly pure carboxylic fatty esters to be used as PCM, Appl. Sci. 8 (7) (2018) 1069, http://dx.doi.org/10.3390/app8071069, http://www.mdpi.com/2076-3417/8/7/1069.

[39] W.H. Organization, Temperature sensitivity of vaccines, 2006, https://apps.who.int/iris/bitstream/handle/10665/69387/WHO_IVB_06.10_eng.pdf;jsessi.